GENERATING RF PULSES USING A NONLINEAR HYBRID LINE

N. S. Kuek, A. C. Liew
Department of Electrical & Computer Engineering, National University of Singapore
4 Engineering Drive 3, Singapore 117583

E. Schamiloglu
Department of Electrical & Computer Engineering, MSC01 1100, University of New Mexico
Albuquerque, NM 87131-001 USA

J. O. Rossi
Associated Plasma Laboratory, National Institute for Space Research, 1758 Astronautas Av.
INPE, Sao Jose dos Campos, Brazil, 12227-010

Abstract

A nonlinear lumped element transmission line (NLETL) that comprises a LC-ladder network where either the capacitors or inductors are nonlinear can be used to convert an input rectangular pulse to a series of RF pulses at the output. This article describes the implementation and demonstration of a high voltage nonlinear hybrid line (NLHL) where both the line components (inductor and capacitors) are nonlinear. Lines with only one nonlinear component have numerous publications in simulation and experimentations whereas NLHL has only a few articles in simulation. There is no report about NLHL being tested to-date according to our knowledge. We have built and tested a NLHL using commercial-off-the-shelf (COTS) components. Instead of using complex pulse forming networks or pulse forming lines, a storage capacitor and a fast semiconductor switch are used to provide an input pulse with good approximation of a rectangular pulse-shape. Experiment results are compared with simulations predicted by the in-house developed NLETL circuit model. Analyses on the voltage modulation and frequency content of the output pulses are carried out. The conditions for producing RF pulses in NLHL and its performance are discussed.

I. INTRODUCTION

There is a recent growing interest in using nonlinear lumped element transmission line (NLETL) for RF generation. NLETL consisting of a LC-ladder network, where only L or C is nonlinear or both are nonlinear, can be used to convert an input rectangular pump pulse to a series of RF oscillations at the output. The most common types of NLETL investigated are the nonlinear capacitive line (NLCL) that comprises nonlinear capacitors and linear inductors [1-2], and the nonlinear inductive line (NLIL) that has nonlinear inductors and linear capacitors [3-4]. The idea of a nonlinear hybrid line (NLHL) where both capacitors and inductors are nonlinear was first proposed by Fallside [5] in 1966 for pulse sharpening and Zucker [6] showed theoretically in 1976 that the NLHL has greater energy compression per stage than a line with either nonlinear capacitance or nonlinear inductance. Gaudet [7] then suggested using the NLHL to achieve RF generation in 2008. To the knowledge of the authors, research work on generating RF pulses using NLHL has been confined to modeling and simulation [8-9]; no experimental result on NLHL has been reported to date. Sanders [10] has intended to build a hybrid line using ferrite beads and capacitors with X7R dielectric (which is expected to exhibit a capacitance decrease of 30%) but he actually checked that the capacitors did not exhibit any significant capacitance changes.

The underlying principle for implementing a NLHL is to create a constant characteristic impedance line to match to the resistive load by finding the right combination of the nonlinear functions C(V) and L(I) of the capacitors and inductors respectively. We adopt here the exponential form of the functions for the nonlinear components that is slightly modified [9] from the one derived by Fallside [5] based on a first-harmonic approximation analysis of nonlinear delay lines. His work actually focuses on pulse sharpening of the rise time, but his equations for a constant impedance line will be used here to study the NLHL for RF generation. For a line to have constant characteristic impedance, the functions L(I) and C(V) must be related so that the characteristic impedance equation

$$Z = \sqrt{\frac{L(I)}{C(Z \cdot I)}} \tag{1}$$

has at least one solution for Z which is independent of I. An example is a line with exponential functions

$$C = C_0 \cdot \left\lfloor x + (1-x) \cdot e^{-q \cdot V} \right\rfloor \tag{2a}$$

$$L = L_0 \cdot \left\lfloor y + (1-y) \cdot e^{-p \cdot I} \right\rfloor . \tag{2b}$$

By assuming $x = y$ and substituting Eq. (2) into Eq. (1)

978-1-4673-5168-3/13/$31.00 ©2013 IEEE

yields (for small values of x and y)

$$Z = \left(\frac{L_0}{C_0}\right)^{1/2} e^{-\frac{1}{2}(pI - qZI)} \quad . \tag{3}$$

Then $Z = Z_0$ exists only if [5]

$$Z_0 = \frac{p}{q} = \left(\frac{L_0}{C_0}\right)^{1/2} \tag{4}$$

where,
C – capacitance as a function of voltage V
L – inductance as a function of current I
C_0 – initial capacitance (at zero voltage)
L_0 – initial inductance (at zero current)
x, y – dimensionless
p, q – nonlinearity factors.

The forms of the equations in Eq. (2) are useful as the asymptotic values are given by the fraction x multiplied by initial capacitance C_0 and the fraction y multiplied by initial inductance L_0.

This article describes the experimental work carried out in building and testing a high voltage NLHL by using commercial-off-the-shelf (COTS) components. The design of the NLHL was made possible by using an NLETL circuit model developed in-house that is well validated by experiments [9]. Results simulated by the NLETL model show fairly good match to the data obtained from the experiments described in this article. In order to better quantify the oscillating pulses, the voltage modulation and the frequency content of the pulses are carefully analyzed using amplitude-cycle and time-frequency plots.

II. DESCRIPTION OF NLHL

The NLHL was built using COTS components and the circuit diagram for setting up the experiment is depicted in Fig. 1. It shows a high voltage (HV) pulse generator circuit connected to a nonlinear LC-ladder network with resistive load R_{load} = 50 Ω. Instead of using a pulse generator that involves a pulse forming network or pulse forming line [2], or one with complex architecture [10], we have implemented a much simpler pulse generator with only a few key components. It comprises a HV power supply, a storage capacitor C_{st} = 1 μF, a fast HV MOSFET semiconductor switch and a current limiting resistor R_{gen} = 50 Ω. This pulse generator can be charged up to 10 kV and produces an output waveform that is almost rectangular in shape. The output pulse duration is adjusted to about 600 ns (controlled by the low voltage trigger pulse) and has a typical rise time of 47 ns and fall time of 44 ns at 6 kV.

The NLHL in Fig. 1 consists of n number of LC sections in which each section contains a single L connected to a single C arranged in a "π" configuration. The nonlinear capacitive element C in the line is a Murata DEBF33D102ZP2A ceramic capacitor rated at 1 nF and 2 kV. For the nonlinear inductive element L in the line a Fair-rite 2944666651 ferrite bead made of NiZn is used. In order to characterize the nonlinear capacitor and nonlinear inductor made from the ferrite bead under dynamic conditions at the time scale of operation of the NLHL, the pulse generator was connected directly to the nonlinear component under test with R_{gen} = 100 Ω. The characterization circuit is illustrated in Fig. 2 where the voltage (V_C or V_L) across the nonlinear component and the current I_{gen} flowing through it are measured.

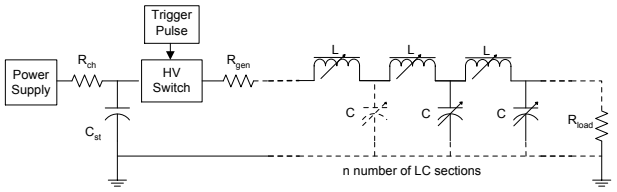

Figure 1. Experimental set-up of a NLHL.

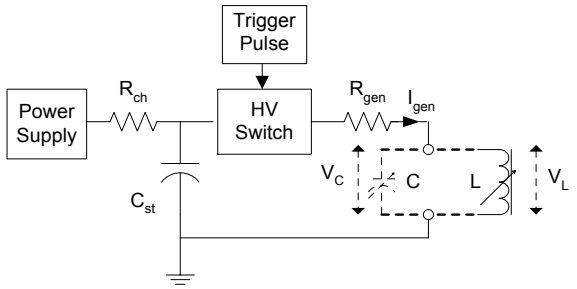

Figure 2. Circuit used for measuring the C-V curve of a nonlinear capacitor and the L-I curve of a nonlinear inductor.

To obtain the C-V curve [11], the pulse generator was used to discharge a 6 kV pulse into the capacitor. The nonlinear differential capacitance can be calculated using

$$C = \frac{dQ}{dV} = \frac{dQ/dt}{dV/dt} = \frac{I_{gen}}{dV_c/dt} \tag{5}$$

where Q is the charge in the capacitor C. The experimental C-V curve was then curve fitted using Eq. (2a). For best fit, the parameters obtained for equation Eq. (2a) are C_0 = 0.995 nF, x = 0.11 and q = 1.583 x 10^{-3} V^{-1}. By using these parameters Eq. 2(a) is also plotted in Fig. 3 with voltage varying up to 6 kV and used in the NLETL model.

Similarly, to obtain the L-I curve [12], an 8 kV pulse was discharge into the ferrite bead from the pulse generator. First, the flux linkage Ψ in the ferrite bead is derived using

$$\Psi(t) = \int V_L(t)dt \,, \tag{6}$$

where V_L is the voltage across the inductor. The characteristic dynamic Ψ-I curve of the nonlinear inductor was plotted and a curve fit was performed on the curve by using an exponential function. The curve fit function for Ψ was then differentiated with respect to current I to obtain the differential inductance L_d that has the exponential form

given in Eq. (2b). For L_d function, the parameters obtained are L_0 = 2.08 μH, y = 0.033, p = 0.169 A^{-1} and Eq. 2(b) is also plotted in Fig. 4 by using these parameters up to a current of 80 A. For comparison, the matching inductance function L_m for L-I curve to go with the capacitance function for C-V curve with Z_0 = 50 Ω can be found by calculating the parameters using Eq. (4). For L_m function, the parameters obtained for Eq. (2b) are L_0 = 2.49 μH, y = 0.11, p = 0.079 A^{-1} and the corresponding equation is also plotted in Fig. 4. The functions L_d and L_m with the exponential form shown in Eq. (2b) are used in the NLETL model for circuit simulations.

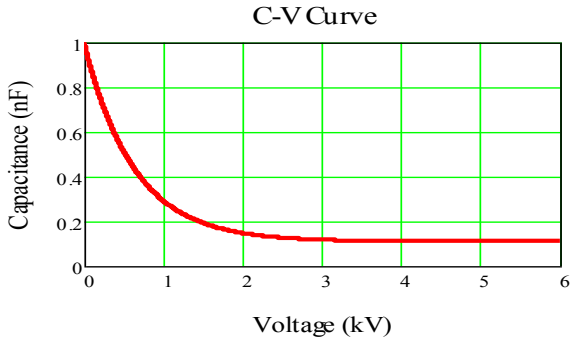

Figure 3. C vs. V curve obtained for the nonlinear capacitor.

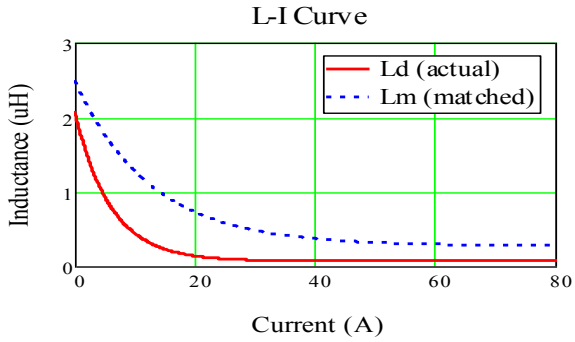

Figure 4. L vs. I curve obtained for the nonlinear inductor.

It should be noted that the measurements for nonlinear inductor were made on the ferrite bead condition with B-H hysteresis curve in the first quadrant. In our case it was observed during experiment that the line with pre-shot reset current to the ferrite beads did not produce excellent sinusoidal-shape oscillations with good amplitudes. Hence, the experiments described in this article were performed with the NLIL without pre-shot reset current.

III. RESULTS OF NLHL

This section analyzes the results of a 20-section NLHL with R_{load} = 50 Ω as described in Fig. 1. The pulse generator is charged to 6 kV and a discharge pulse of 600 ns duration with approximately rectangular shape is injected into the NLHL.

We use here the average peak load power P_{ave} and voltage modulation depth (VMD) as defined in [11]. In order to find the load that best matches to the line in terms of P_{ave}, a parameter sweep on the load was performed using the NLETL simulation model. The load of 50 Ω was chosen as it gives peak power near to the maximum point in the sweep. The measured load voltage indicates a fairly good agreement with the simulated result (by means of L_d) as shown in Fig. 5. The simulated matched case using L_m is also depicted in Fig. 5 for comparison.

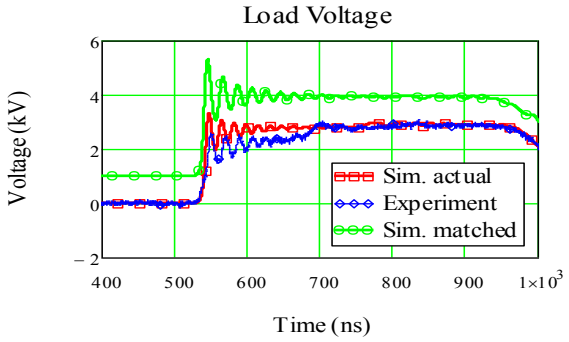

Figure 5. Load voltage vs. time for a 20-section NLHL. The simulated matched case is offset by +1 kV for clarity.

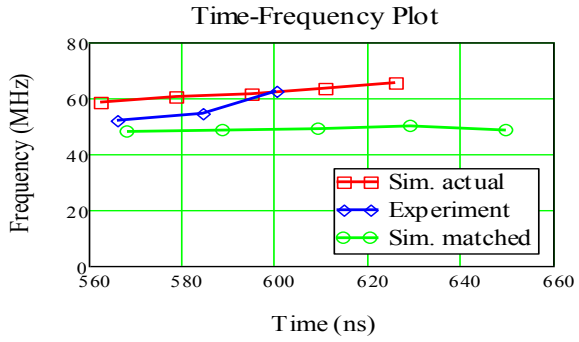

Figure 6. Voltage oscillation frequency vs. time for a 20-section NLHL.

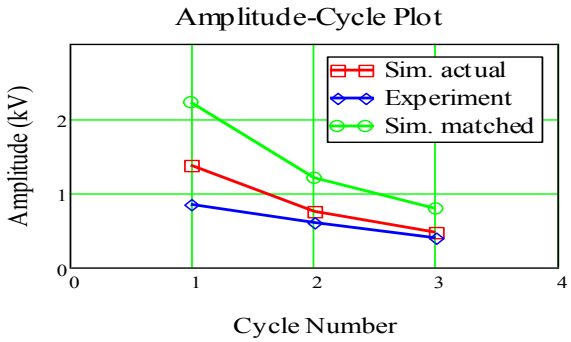

Figure 7. Peak-to-trough oscillation amplitude vs. oscillation cycle number for a 20-section NLHL.

It is of interest to understand how the frequency of the oscillations changes with time rather than performing a FFT on the output voltage pulse. The frequency of each cycle in the oscillations is calculated and plotted against

the time when the cycle ends. This time-frequency plot shows the number of cycles of oscillations by simply counting the number of points plotted. The time-frequency plots for the simulation and experimental results are shown in Fig. 6. The frequencies obtained for the simulated actual case and the experiment are around 60 MHz and 55 MHz, respectively. The simulated matched case has frequencies in the region of 50 MHz.

To see the quality of the load voltage modulation, the peak-to-trough oscillation amplitude V_{pt} is obtained for the first three cycles and is shown in the amplitude-cycle plot in Fig. 7. The VMDs as defined in [11] for the simulated actual case and experiment are VMD_{Ld} = 859 V and VMD_{expt} = 615 V, respectively. The simulated matched case has VMD_{Lm} = 1398 V which is higher as expected due to the ideally matched conditions specified in Eq. (1) to Eq. (4).

The effects of the amplitude of the input pulse were also studied by varying the pulse generator voltage from 5 kV to 8 kV in steps of 1 kV. The measured load voltages are depicted in Fig. 8. The time-frequency plot and amplitude-cycle plot are shown in Fig. 9 and Fig. 10, respectively. As the voltage increases from 5 kV to 8 kV, the oscillation frequencies increase from around 50 MHz to 70 MHz and the oscillation amplitudes also show considerable increases.

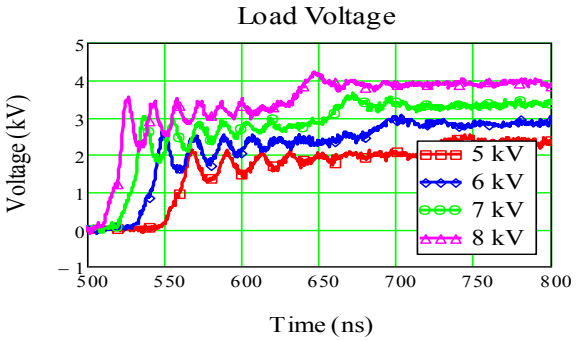

Figure 8. Exp.: Load voltage vs. time for a 20-section NLHL for different pulse generator voltages.

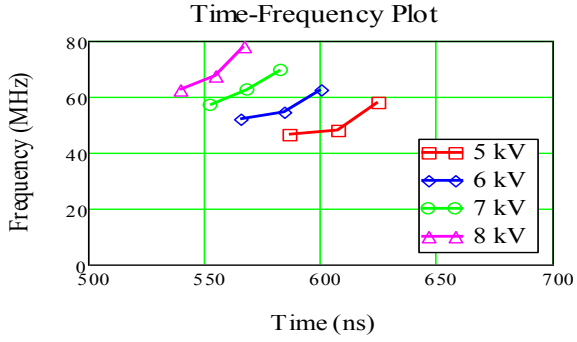

Figure 9. Exp.: Voltage oscillation frequency vs. time for a 20-section NLHL for different pulse generator voltages.

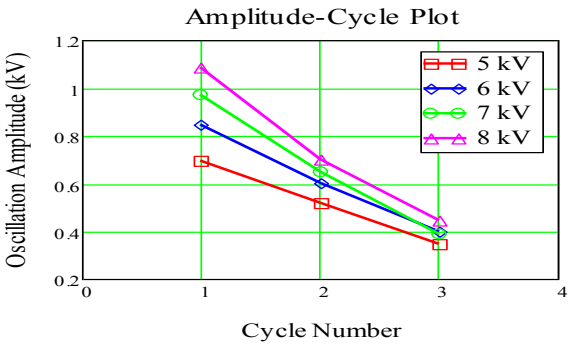

Figure 10. Exp.: Peak-to-trough oscillation amplitude vs. oscillation cycle number for a 20-section NLHL for different pulse generator voltages.

IV. CONCLUSIONS

We have demonstrated using COTS components that a simple pulse generator comprising a storage capacitor and a fast MOSFET semiconductor switch can be used to drive a NLHL to produce RF oscillations. Although a matched L-I curve to the C-V curve will in theory produce oscillation with good VMD, it is shown in this article that an unmatched case is also capable of producing RF oscillations albeit with reduced VMD. The VMD in the unmatched case can be increased by increasing the amplitude of the input driving pulse which also at the same time increase the oscillation frequency. It should be noted that the equivalent series resistor (ESR) of the nonlinear capacitors used in the experiment is estimated to be about 2 Ω. Reducing the ESR by a factor of 2 or more (if better nonlinear capacitors with reduced dielectric losses are employed) will substantially improve the VMD.

V. ACKNOWLEDGMENTS

J. O. Rossi acknowledges his sponsor, USAF SOARD for their support (contract number no. FA9550-13-1-0132).

VI. REFERENCES

[1] M. P. Brown and P. W. Smith, "High power, pulsed soliton generation at radio and microwave frequencies," *Proc. 11th IEEE Int. Pulsed Power Conf.* (Baltimore, MD, 1997), pp. 346-354.

[2] J. D. C. Darling and P. W. Smith, "High power pulse burst generation by soliton-type oscillation on nonlinear lumped element transmission lines," *Proc. 17th IEEE Int. Pulsed Power Conf.* (Washington, DC, 2009), pp. 119-123.

[3] A. M. Belyantsev, A. I. Dubnev, S. L. Klimin, Yu. A. Kobelev and L. A. Ostrovskii, "Generation of radio pulses by an electromagnetic shock wave in a ferrite loaded

transmission line," *Tech. Phys.*, vol 40 (8), pp. 820-826 (1995).
[4] N. Seddon, C.R. Spikings, and J.E. Dolan, "RF pulse formation in nonlinear transmission lines," *Proc. 16th IEEE Int. Pulsed Power Conf.* (Albuquerque, NM 2007), pp. 678-681.
[5] F. Fallside and D.T. Bickley, "Nonlinear delay line with a constant characteristic impedance," *Proc. IEE*, vol. 113, 263-270 (1966).
[6] O. S. F. Zucker and W. H. Bostick, "Theoretical and practical aspects of energy storage and compression", in *Energy Storage, Compression and Switching* edited by W.H. Bostick, V. Nardi and O.S.F. Zucker. New York: Plenum Publishing Corp., 1976, pp. 71-93.
[7] J. Gaudet, E. Schamiloglu, J. O. Rossi, C. J. Buchenauer, and C. Frost, "Nonlinear transmission lines for high power microwave applications – A survey," *Proc. 28th IEEE Int. Power Mod. Conf. and 2008 High Voltage Workshop* (Las Vegas, NV, 2008), pp. 131-138.
[8] J. O. Rossi, P. N. Rizzo and F. S. Yamasaki, "Prospects for applications of hybrid lines in RF generation," *Proc. of 2010 IEEE Int. Power Modulator and High Voltage Conf.* (Atlanta, GA, 2010), pp. 632-635.
[9] N. S. Kuek, A. C. Liew, E. Schamiloglu and J. O. Rossi, "Circuit modeling of nonlinear lumped element transmission lines including hybrid lines," *IEEE Trans. Plasma Sci.*, vol. 40, no. 10, pp. 2523-2534, Oct. 2012.
[10] J. M. Sanders, Y. H. Lin, R. Ness, A. Kuthi and M. Gundersen, "Pulse sharpening and soliton generation with nonlinear transmission lines for producing RF bursts," *Proc. of 2010 IEEE Int. Power Modulator and High Voltage Conf.* (Atlanta, GA, 2010), pp. 604-607.
[11] N. S. Kuek, A. C. Liew, E. Shamiloglu and J. O. Rossi, "Generating Oscillating Pulses Using Nonlinear Capacitive Transmission Lines," Proc. of *2012 IEEE Int. Power Modulator and High Voltage Conf.* (San Diego, CA, June 2012), pp. 231-234.
[12] N. S. Kuek, A. C. Liew, E. Schamiloglu and J. O. Rossi, "Nonlinear inductive line for producing oscillating pulses," *4th Euro-Asian Pulsed Power Conf. / 19th Int. Conf. on High-Power Particle Beams* (Karlsruhe, Germany, October 2012), in press.